*powders*

MDPI

*Article*

# Investigation of the Influence of the Mixing Process on the Powder Characteristics for Cyclic Reuse in Selective Laser Sintering

**Tom Eggers *, Hendrik Rackl and Frank von Lacroix**

Volkswagen AG Wolfsburg, Berliner Ring 2, 38440 Wolfsburg, Germany
* Correspondence: tom.eggers1@volkswagen.de

**Abstract:** Selective laser sintering (SLS) with polymers is currently at the transition to the production of functional components and thus holds great potential to revolutionize conventional production processes. Nevertheless, the application capability is confronted by newly defined requirements regarding reliability and reproducibility. In order to fulfil the requirements and to increase the process stability, the ageing mechanisms in polymers are compensated by recycling strategies. This involves fraction-based mixing of a defined ratio of new powder with recycled powder. Basically, fraction-based mixing must be preceded by the selection of suitable mixing parameters. The work focused on the influence of the mixing process on the powder characteristics for cyclic reuse in SLS. With regard to the powder characteristics, the particle shape and particle size distribution as well as the bulk and tap density of the powder were investigated. The authors found an influence of the mixing process with increasing mixing time on the powder characteristics of a black polyamide 12 sintering material. A mixing time of 1 h and a mixing intensity of 15 rpm proved to be potentially effective for achieving a gentle and homogeneous mixing of the powders.

**Keywords:** additive manufacturing; selective laser sintering; polymers; powders; mixing process; particles; powder density; agglomerates; interparticle forces



**Citation:** Eggers, T.; Rackl, H.; von Lacroix, F. Investigation of the Influence of the Mixing Process on the Powder Characteristics for Cyclic Reuse in Selective Laser Sintering. *Powders* **2023**, *2*, 32–46. https://doi.org/10.3390/powders2010003

Academic Editor: Paul F. Luckham

Received: 16 November 2022
Revised: 29 November 2022
Accepted: 4 January 2023
Published: 10 January 2023



## 1. Introduction

### *1.1. Process Technology of Selective Laser Sintering and Material Properties*

Selective laser sintering (SLS) with polymers represents the additive manufacturing process that is currently in transition between its application in prototyping to full manufacturing technology for functional components. In addition to the suitability of the process for future industrial application, the process offers the potential of integration into series production. SLS is a powder-based process in which components are generated by the layer-wise application and selective solidification of mainly polymer materials by using heat input. Taking into account minimal distances between the components, the building volume can be fully utilized. The surrounding, non-consolidated powder can be reused [1–3]. A restriction of the process is that the powder material used is subject to a combination of material ageing processes, which are each reflected as impacts on the specific characteristics of the material [2,4–9]. Thus, the powder in SLS is considered to be the decisive quality criterion [10]. The processability of the polymer is influenced by the material properties. The material properties are divided into intrinsic and extrinsic properties [11–13]. The extrinsic properties include the particle shape and particle size or particle size distribution (PSD) and flowability of the powder. These properties are decisive factors influencing the behavior of the powder in the SLS process [11,13]. In a cohesive powder, there are interactions between the particles, as a result of which the free flow of the powder is influenced [11,14]. The interparticle forces are caused by forces that keep the particles together, such as gravitational forces, mechanical interlocks and van der Waals interactions [11,14–16]. A spherical particle shape favors the flowability and

applicability of the powder in the SLS process [11–13]. Mys et al. [17] listed suitable particle shapes for use in SLS. In order to achieve the desired component properties, SLS powders should ensure a sufficient packing density of the powder layers [11–13]. Furthermore, environmental conditions such as temperature and humidity influence the flow behavior in that the humidity absorbed by the powder causes hydrogen bonds to form between the particles [14,18,19].

### *1.2. Approaches of Fraction-Based Mixing for Recycling Powders in SLS*

With regard to a consistent powder and component quality, the ageing mechanisms in polymers during SLS are compensated by recycling strategies [4]. Actions for the quality management of materials with regard to ageing mechanisms are listed in [11,20]. Gibson et al. [2] described the fraction-based mixing of a defined ratio of recycled powder with new powder. For this purpose, the powder materials from the overflow and the feed unit as well as the powder from the building volume of the SLS system are differentiated. The different powder fractions are to be separated from each other using lists and the use of different containers according to their ageing status [4,11]. Labeling the containers with barcodes or radio-frequency identification chips is also conceivable [21]. The reason for the separation of the powder fractions is that the powder is exposed to different temperature profiles during the SLS process. Due to the low temperatures in the overflow and feed unit, the powder from the overflow and feed unit differs only marginally from new powder. The non-solidified powder from the building volume is exposed to higher thermal impacts and is processed in a particle sorting method to break up or sort out particle agglomerates. Fraction-based mixing ratios of the various powders are then determined [2]. Gibson et al. [2] mentioned a mixing ratio of one third virgin powder, one third powder from the overflow and feed unit, and one third powder from the building volume. Further studies [2,4,7,11,22–24] identified mixing ratios of 30% to 50% virgin with recycled powder in the case of polyamide 12. Depending on the specific melt viscosity of the powder fractions, more precise mixing ratios can be set using the melt index measurement [2,7,11,20,25–33]. In this regard, there are various studies that focus on the determination of limit values for material quality and establish an evaluation system. This makes it possible to predict the time at which ageing effects occur in polymers in the course of increasing molecular weight [7,25–27,34].

In this regard, Gibson et al. [2] described the homogenization of the powder fractions in a mixing process. Homogenization occurs when each powder sample represents the entirety of the powder [35]. In Mwania et al. [36]'s study, the different types of mixing mechanisms and mixing parameters were listed, which influence the mixing of powder fractions with different powder characteristics. These include particle size, PSD, particle shape, particle density and cohesiveness [11,37]. The mixing parameters that influence the homogeneity of the powder mixture include the mixing duration and mixing intensity, the filling volume of the mixer and the shaping of the mixer [37,38]. Furthermore, the inconsistent powder characteristics influence the homogenization of the powder fractions [37]. Sommer [39], Weinekötter and Gericke [40] and Stieß [38] present the forms and properties of solid mixers. Deveswaran et al. [37] listed requirements for a mixer for homogenization powders in SLS:

- Time-saving mixing;
- Gentle mixing of the powder;
- Dust-proof design of the mixer;
- Low-effort removal of the powder and cleaning of the mixer;
- Design of the mixer for varying powder volumes.

According to Weinekötter and Gericke [40], free-fall mixers are particularly suitable for the homogenization of a powder mixture. In addition, possible segregation effects of particles are lower with this mixer. Furthermore, free-fall mixers have the least mechanical influence on the mixture and thus avoid deterioration to the mixture [40]. According to Bhoite et al. [41], Weber [42] and Blümel [43], a tumbling mixer is a free-fall mixer and represents a process that is gentle on the mixed material with the most homogeneous

mixing possible. Fahr and Voigt [44] attested that this mixer has low shear forces, which has minimal effects on the structural integrity of powder materials for use in additive manufacturing.

According to Hogg [45], mixing is favored by an increased speed of the mixer. Furthermore, long mixing times result in a more homogeneous mixing of the powders. From Poux et al. [46] a suitable mixing duration of 2 min to 10 min is given. A short mixing time was confirmed by Blümel [43]. Mayer-Laigle et al. [47] demonstrated that with a Turbula T2F tumbling mixer, homogeneous mixing of two different materials is achieved after only few rotations of the mixer, regardless of the mixing intensity. Ferraris [48] suggested a mixing intensity of 5 rpm to 25 rpm. A low mixing intensity for sufficient mixing was also confirmed by Blümel [43]. Investigations by Shad et al. [49] with a Turbula T10B tumbling mixer using a powder mixture of metallic powders and flow aids showed that both long mixing times and high mixing intensities lead to homogenization of the powder materials. It is shown that a higher mixing energy (consisting of mixing time and intensity) is generally effective, regardless of how this energy is provided. A mixing time of 1 h and a mixing intensity of 44 rpm was used for the investigations carried out [49].

Furthermore, an increased filling volume of the mixer results in a lower mobility and mixing of the particles [45]. Studies by Mwania et al. [36] with similar polymer particles identified a filling level of 50% to 75% for sufficient mobility and mixing of the particles. In Mayer-Laigle et al. [47]'s study, homogeneous mixing was achieved at a filling level of 50%. The tendency to segregation depends on the size, shape and packing density of the particles [46,50]. In addition, small particles tend to align with each other during the mixing process, while larger particles agglomerate [46]. Compared with irregularly shaped particles, spherical particles agglomerate more [46,50].

### *1.3. Aim of the Article*

Material ageing processes in polymers limit the industrial application of SLS [2,5,11]. The influence of the specific material characteristics affects the quality and reproducibility of the component properties as well as the process stability of the SLS [2,4,5,11,24,51–53]. To compensate these ageing mechanisms, it is common practice to refresh powder already used in the process by adding new powder [4,11,24,51,52]. Gibson et al. [2] describe the approach of fraction-based mixing of a defined ratio of virgin to recycled powder. Previous studies focus on the mixing of various bulk materials with regard to suitable mixing parameters for homogeneous mixing, but not on the mixing of powder fractions, in particular polyamide 12, for cyclic use in SLS. Whether the powder properties are influenced as a result of homogenization has not yet been clarified. Therefore, the selection of suitable mixing parameters for the application at hand has to be made. The aim of the work was to investigate the influence of the mixing parameters on the powder characteristics and to identify parameters that are gentle on the mixed material. The focus of the investigation was on the particle shape and PSD as well as on the bulk and tap density of the powder.

## 2. Materials and Methods

### *2.1. Sinter Material*

In this work, the powdered polyamide 12 sintering material LUVOSINT PA12 9270 BK from the manufacturer Lehmann & Voss & Co. KG (Hamburg, Germany) is used. The sintering material was stored airtight at 23 °C and 50% relative humidity and protected from ultraviolet radiation. The choice of material is justified by the fact that polyamide 12 is the most commonly used sintering material in SLS [2,11,54,55]. Based on the information provided by the manufacturer, the material has a specific gravity of 1.02 g/cm$^3$ and a bulk density of 0.40 g/cm$^3$.

### *2.2. Mixing Technology*

The powders were mixed using a Turbula T10B tumbling mixer from the manufacturer WAB AG (Muttenz, Switzerland). The tumbling mixer offers a process that is gentle on the

material to be mixed with the most homogeneous mixing possible [38–43,56]. Four different mixing intensities (15 rpm, 23 rpm, 32 rpm, 44 rpm) were used. The selection of the mixing intensities results from the basic settings and the transmission ratio of the drive. Mixing times from 30 min to 96 h are investigated. The selection of mixing times results from a compromise between sufficient mixing of the powder and, at the same time, the gentlest possible mixing. The short mixing times are in accordance with the studies [43,46,47]. To illustrate possible effects of mixing time on the powder, both short and long mixing times were selected. Mixing containers with a capacity of 500 mL were used to investigate the powder characteristics in the mixing process. A percentage filling level of 75% was applied. This filling level is confirmed by investigations by Mwania et al. [36] with polymer particles. As the mixer is a free-fall mixer [41–43], there are no grinding bodies inside the mixing containers.

### *2.3. Classification of Powder Density*

To determine the powder characteristics, the bulk density and tap density were determined under controlled environmental conditions of 23 °C and 50% relative humidity. The quotient of tap density and bulk density is called the Hausner factor [14,57,58]. As the Hausner factor only indicates the ratio of the two values, the Hausner factor is not used to describe the flow behavior. Spierings et al. [59] confirmed this approach. Furthermore, studies show a correlation between powder flowability and bulk density [43,60–62]. The bulk density was determined according to DIN EN ISO 60:2000-01 [63] using a defined hopper from the manufacturer Landgraf Laborsysteme HLL GmbH. For the measurement, a powder amount of 110 mL to 120 mL is used, which flows through a hopper into a measuring cylinder. The bulk density was calculated from the ratio of the mass of the powder in the measuring cylinder and the volume of the measuring cylinder. The determination of the tap density was carried out according to the procedure described in DIN EN ISO 787-11:1995-10 [64] with a tap volumeter from the manufacturer Landgraf Laborsysteme HLL GmbH (Langenhagen, Germany). The measuring cylinder was filled up to a measuring volume of 200 $\pm$ 10 mL with the powder. The powder was dried previously by a drying oven of the type TR 120 from Nabertherm GmbH (Lilienthal, Germany). After the compression processes of 1250 revolutions of the camshaft, the volume after the last compression process is taken as the final volume. The tap density calculated from the ratio of the mass of the powder in the measuring cylinder and the noted filling volume. The corresponding mass of the powder in the measuring cylinder was determined by a scale of the type EW 4200-2 NM from KERN&Sohn GmbH (Balingen-Frommern, Germany). The mass was determined at 23 °C and 50% relative humidity. To achieve a higher statistical significance, three determinations of the bulk density and tap density of the powder were carried out and the arithmetic average was formed, contrary to the specifications in DIN EN ISO 60:2000-01 [63] and DIN EN ISO 787-11:1995-10 [64].

### *2.4. Particle Analysis*

For the analysis of the particle shape and PSD by a dynamic image analysis according to ISO 13322-2:2021-12 [65] the particle analyzer of the type Camsizer XT of the manufacturer Retsch Technology GmbH (Haan, Germany) is used. For the analysis of the particles, measurements with five million recorded particles in each case were carried out. As a result of the measurements, the sphericity and aspect ratio are available as mean values. In addition, the D10, D50, and D90 values as well as the PSD were output. This measurement does not provide for a standard deviation. Regarding the particle shape, the focus was on sphericity and aspect ratio. The maximum value for sphericity and aspect ratio was 1 [11,66]. The particles were analyzed under controlled environmental conditions of 23 °C and 50% relative humidity.

### *2.5. Scanning Electron Microscope*

The scanning electron microscopic (SEM) images of the sintering material are taken with a Tescan Mira 3 SEM system from Tescan GmbH (Dortmund, Germany). The microscope was operated with an acceleration voltage of 15 kV, detection was carried out via secondary electrons. The samples were first sputtered with gold for 40 s so that the particle surface was electrically conductive [67].

## 3. Results and Discussion

### *3.1. Characteristics of the Used Sinter Material*

The PSD curve of the used sintering material is shown in Figure 1. The distribution curve appears broad and symmetrical and has a mono-modal shape [11–13]. Table 1 lists the powder characteristics of the used sintering material. The bulk density deviated from the tap density by approx. 28.8%.

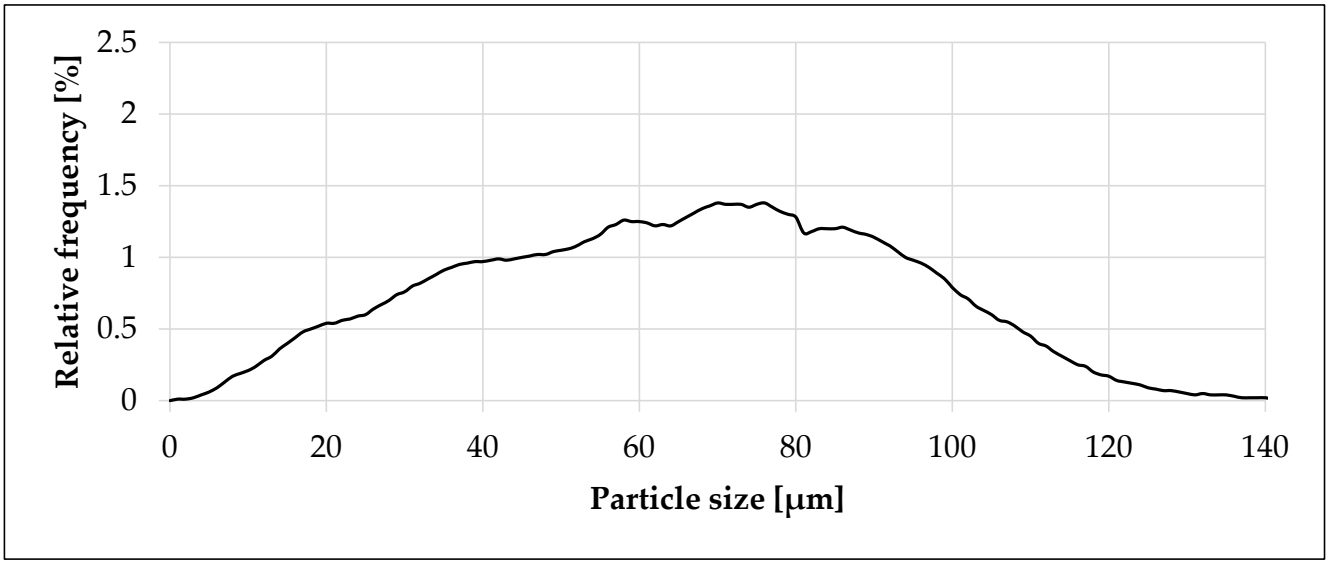


**Figure 1.** Particle size distribution of the used sinter material. The analysis of the particle size distribution includes the frequency of occurrence over the respective particle size, which is shown on the *x*-axis. Determined with Camsizer XT.

**Table 1.** Characteristics of the investigated sinter material.

| Attribute | Average | Standard Deviation |
|---|---|---|
| Bulk density | 0.3906 g/cm$^3$ | 0.0030 g/cm$^3$ |
| Tap density | 0.5033 g/cm$^3$ | 0.0033 g/cm$^3$ |
| D10 | 28.20 µm | - |
| D50 | 66.30 µm | - |
| D90 | 100.00 µm | - |
| Sphericity | 0.838 | - |
| Aspect ratio | 0.710 | - |

The distribution of particle size within the sintering material is confirmed in Figure 2. The particle morphology of the powder appears irregular and fractured, which is reflected in the sphericity and aspect ratio (Table 1) [11,17]. Sharp fracture edges are visible on the particles.

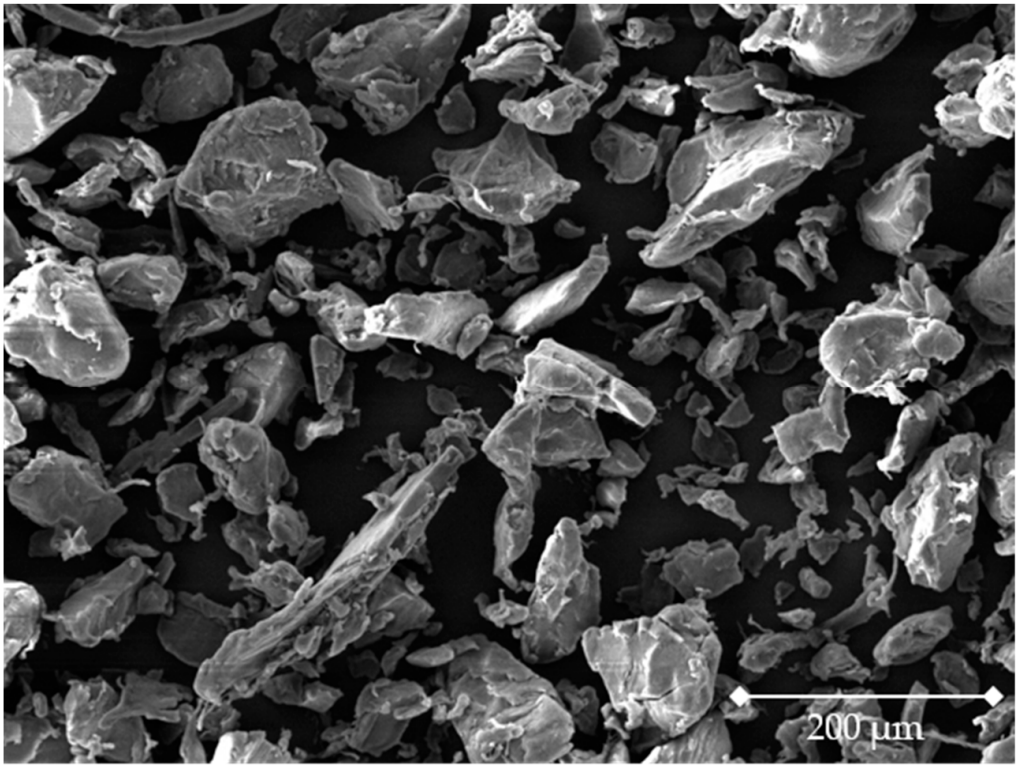


**Figure 2.** SEM image of the used sinter material. Produced with Tescan Mira 3 at 150× magnification.

### *3.2. Influence on Particle Shape and Particle Size Distribution*

The influence of the mixing process on the sphericity and aspect ratio is shown in Figures 3 and 4. The curves showed a sinusoidal function. Sphericity and aspect ratio increased with increasing mixing energy. However, the mixing energy decreased when switching from one mixing duration to the next mixing duration in the diagrams, since there is then again a low mixing intensity. The mixing intensity has the stronger influence on the form factors than the mixing time. The minimum sphericity was 0.837 and was achieved at a mixing time of 0.5 h and a mixing intensity of 23 rpm. In contrast, the maximum sphericity was 0.845 and was achieved at a mixing intensity of 44 rpm and mixing durations of 4 h and 96 h in both cases. This corresponds to a maximum percentage deviation of approx. 1% compared with the sphericity of the reference material (Table 1). The minimum aspect ratio was 0.703 at a mixing time of 96 h and a mixing intensity of 15 rpm. In contrast, the maximum aspect ratio was 0.716 and was achieved at a mixing time of 4 h and mixing intensities of 23 rpm and 44 rpm. This corresponds to a maximum percentage deviation of approx. 1% compared with the reference material (Table 1). Furthermore, the percentage deviation within the series of tests for the sphericity was a maximum of approx. 1% and for the aspect ratio a maximum of approx. 2%. In particular, low mixing energies lead to a change in the form factors of less than 1%.

The influence of the mixing process on the characteristic values of the PSD is shown in Figure 5. Especially at low mixing times of 0.5 h and 1 h, independent of the mixing intensity, the particle sizes were influenced by less than 2%. Basically, an increase in particle size with increasing mixing energy could be observed. In particular, mixing durations in the range of 48 h and 96 h resulted in an increase in particle size. Here, at a mixing duration of 96 h and a mixing intensity of 23 rpm, a percentage increase of up to 4% (D90) occurred compared with the reference material (Table 1). The fine particle fraction is increased with increasing mixing energy to a maximum value of 34.90 µm-D10. This represents a percentage increase of approx. 23.8% compared with the reference material (Table 1). While the D90-fraction increased by 3.3% starting from the reference material up to the maximum

mixing energy (96 h, 44 rpm), the increase in the D50-fraction was approx. 9%. For the D10-fraction, the increase was 20.2%.

The SEM images of the particles at different mixing parameters shown in Figure 6 confirm the observations in Figure 5 of the particle size increase with rising mixing energy. With increasing mixing time and mixing intensity, particle agglomerates and breakouts from the particles were increasingly present compared with the reference material (Figure 2). The particle surface appeared more damaged, deformed, and rougher than the reference material or the powders mixed at lower mixing energies. In addition, with increasing mixing energy, an intensified formation of satellites occurred, in which small particles attached themselves to larger particles. The increase in sphericity and aspect ratio seen in Figures 3 and 4 is not evident in the SEM images.

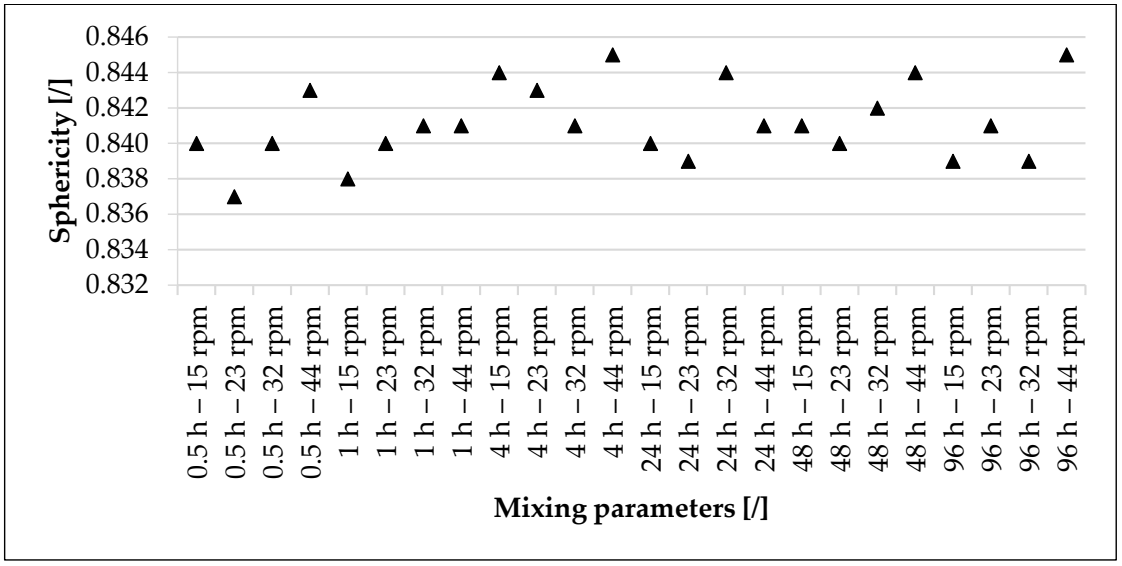


**Figure 3.** Influence of the mixing process on the sphericity of the sinter material. Six mixing durations are considered, each with four mixing intensities. Determined with Camsizer XT.

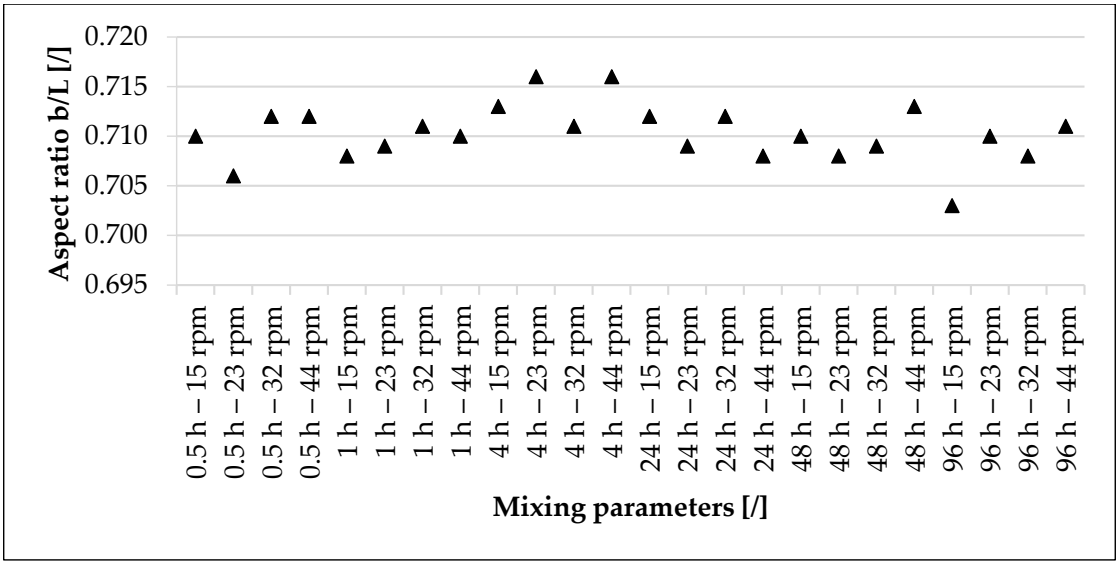


**Figure 4.** Influence of the mixing process on the aspect ratio of the sinter material. Six mixing durations are considered, each with four mixing intensities. Determined with Camsizer XT.

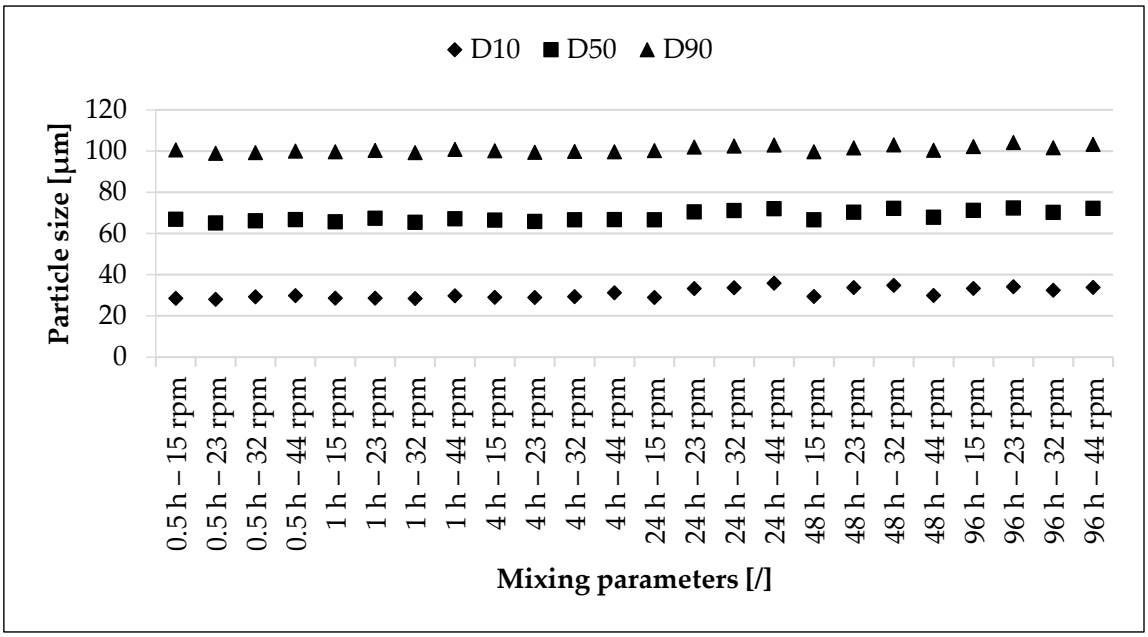


**Figure 5.** Influence of the mixing process on the characteristic values of the particle size distribution. Six mixing durations with four mixing intensities in each case are considered. Determined with Camsizer XT.

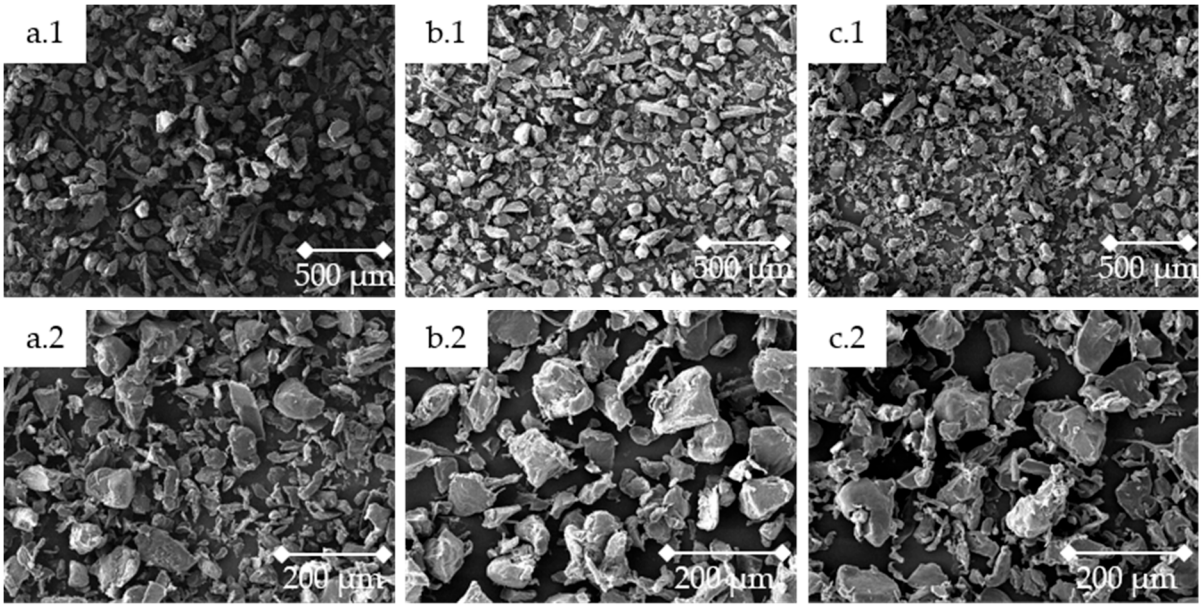


**Figure 6.** SEM images of the particles of used sinter material: (**a.1**,**a.2**) 1 h—15 rpm at 46× and 150× magnification; (**b.1**,**b.2**) 1 h—44 rpm at 48× and 168× magnification; (**c.1**,**c.2**) 96 h—44 rpm at 48× and 168× magnification. Determined with Tescan Mira 3.

### *3.3. Influence on the Powder Density*

The influence of the mixing process on the powder density is shown in Figures 7 and 8. The bulk density and tap density decreased with increasing mixing time. At high mixing energies, the mixing process had a stronger effect on the bulk density than on the tap density. With reference to Figure 7, a decrease in bulk density occurred from a mixing duration of 4 h, which lies outside the standard deviation of the reference material (Table 1). Based on a mixing time of 4 h and a mixing intensity of 44 rpm, there was a percentage decrease of approx. 1.6% compared with the reference material. At the same mixing intensity and a

mixing time of 96 h, there was a percentage decrease of approx. 8.8% compared with the reference material. The decrease in bulk density is primarily caused by an increasing mixing time. In addition, the influence of the increasing mixing intensity occurred from a mixing duration of 48 h upwards. Based on a mixing time of 96 h, the bulk density decreased from a mixing intensity of 15 rpm (0.3718 g/cm$^3$) to 44 rpm (0.3561 g/cm$^3$) by approx. 4.2%. In contrast, the change in bulk density related to a mixing duration of 1 h from a mixing intensity of 15 rpm (0.3872 g/cm$^3$) to 44 rpm (0.3866 g/cm$^3$) was approx. 0.1%.

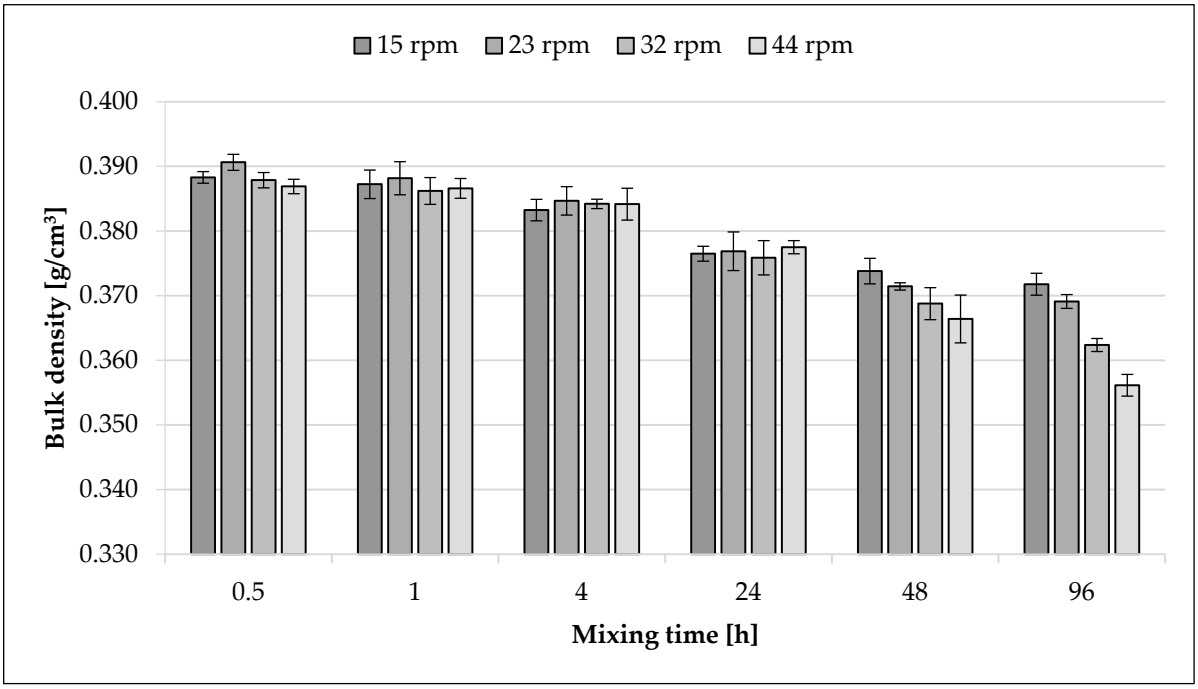


**Figure 7.** Influence of the mixing process (time and intensity) on the bulk density. Six mixing durations are considered, each with four mixing intensities.

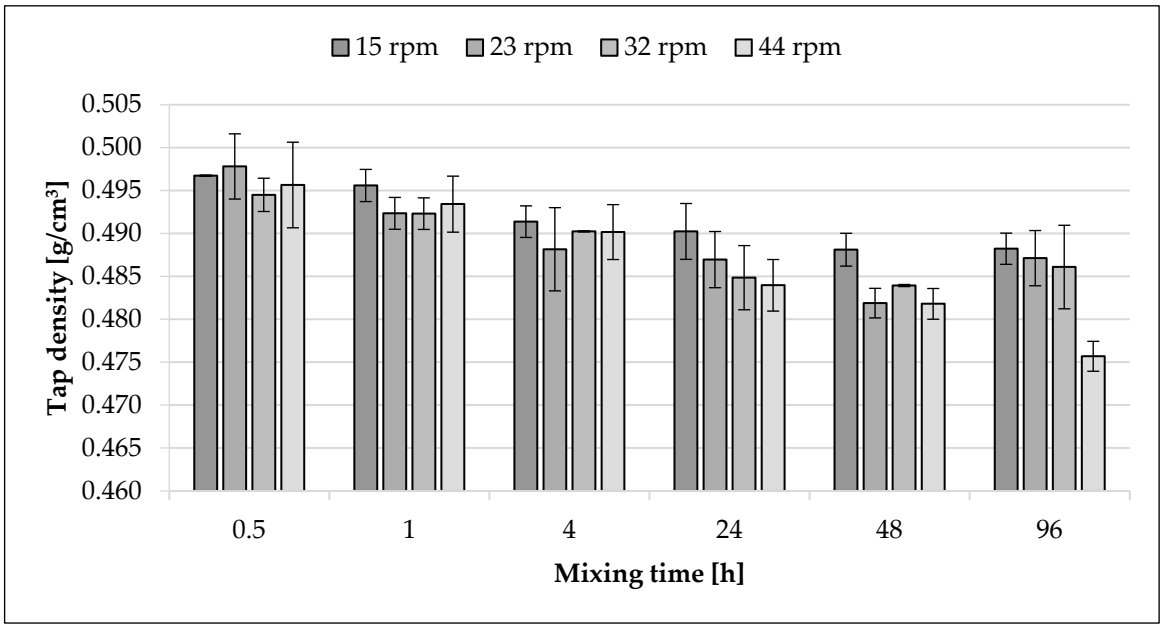


**Figure 8.** Influence of the mixing process (time and intensity) on the tap density. Six durations are considered, each with four mixing intensities.

Similar to the bulk density, the tap density decreased with increasing mixing time. After a mixing time of 0.5 h, the tap densities were partly outside the tap density of the reference material, under consideration of the standard deviation. From a mixing duration of 1 h upwards, all mixing intensities resulted in a lower tap density than that of the reference material, under consideration of the standard deviation. At a mixing time of 1 h and a mixing intensity of 15 rpm (0.4956 g/cm$^3$), there was a percentage decrease in the tap density of approx. 1.5% compared with the reference material. Based on a mixing time of 4 h and a mixing intensity of 44 rpm (0.4902 g/cm$^3$), there was a percentage decrease of approx. 2.6% compared with the reference material. With the same mixing intensity and a mixing time of 96 h (0.4757 g/cm$^3$), there was a percentage decrease of approx. 5.5% compared with the reference material. Basically, the decrease of the tap density is primarily caused by an increasing mixing time. In addition, the influence of the increasing mixing intensity occurred from a mixing duration of 24 h upwards. Based on a mixing time of 96 h, the tap density decreased from a mixing intensity of 15 rpm (0.4882 g/cm$^3$) to 44 rpm by approx. 2.5%.

### *3.4. Discussion*

The influence of the mixing process on the powder characteristics of the used sintering material was investigated. Although the used tumbling mixer is a low shear mixing technology [41–44], it was shown that the sphericity and aspect ratio increased with rising mixing energy (Figures 3 and 4). This could be due to the sharp edges of the particles being rounded by the contact of the particles during the mixing process. As a result, a high mixing energy leads to a stronger rounding of the particles. Furthermore, the mixing intensity had a stronger influence on the form factors than the mixing time. However, the increase in form factors may not be decisive due to the small percentage changes of about 1%.

The increase in particle size with rising mixing energy shown in Figure 5 is possibly due to agglomeration of the particles as a result of mechanical interlocking of the individual particles [11,14,68,69]. The SEM images of the particles at different mixing parameters shown in Figure 6 confirm the observations of the increase in particle size recorded in Figure 5. The increased formation of satellites also resulted in a shift of the particle size towards higher particle sizes. Although the form factor analysis indicates a rounding of the particles, the particles in the SEM images appeared damaged, deformed, and agglomerated compared with the reference material (Figure 2) or the powders mixed at low mixing energies (Figure 6). Furthermore, agglomeration is favored by the previously noted rounding of the particles in the mixing process [46,50]. This assumption is supported by the circumstance that at low mixing energies there is no measurable rounding of the particles and an increase in particle size. The use of the tumbling mixer as well as the procedure, the number of samples, and sampling of the test methods carried out reduces the occurrence of segregation effects of small and large particles. Therefore, the results obtained can be considered valid.

Furthermore, the influence of the mixing process on the powder density, described by the bulk density and tap density, is shown in Figures 7 and 8. Although the previously recorded rounding of the particles should result in better powder flowability [11–14], the density of the powder decreased with increasing mixing energy. The decrease in bulk and tap density is due to the mechanical interlocking of single particles, the agglomeration of these and the damage of the particles (Figures 5 and 6) [11,14,68,69]. The decrease in bulk and tap density indicates increasing interactions between the particles, so that the powder becomes more cohesive with increasing mixing energy [11,14]. Based on the sintering material as well as the form factors and SEM images (Figures 5 and 6), the decrease in bulk and tap density is primarily due to adhesive forces and mechanical interlocking of the powder [11,14–16,70]. In addition, electrostatic forces between the particles are also conceivable, which lead to the formation of agglomerates with increasing mixing energy [71,72], even though these forces were not studied in this work. Furthermore,

the mixing duration has a greater influence on the bulk and tap density than the mixing intensity. The influence of the mixing intensity only became apparent from a mixing duration of 48 h. This observation is due to the low density of polymer powders [11]. In addition, the mixing process has a stronger effect on the bulk density than on the tap density. This is due to the characteristic of the determination of the tap density according to DIN EN ISO 787-11:1995-10 [64]. While the powder flows freely when determining the bulk density, the powder is excited when determining the tap density. This could dissolve initial agglomerates and mechanical interlocking of the particles caused by the mixing process. Moreover, the powder is strongly compacted, so that the influence on the powder density becomes visible especially when the powder flows freely. An influence of environmental conditions such as temperature and humidity on the flow behavior is not to be expected [14,18,19]. This is due to the mixing process and the powder analysis being carried out under constant environmental conditions of 23 °C and 50% relative humidity.

### *3.5. Identification of Suitable Mixing Parameters*

Based on the findings, it is obvious that high mixing energies have an effect on the powder characteristics. In particular, long mixing times should be avoided in order to ensure gentle mixing of the polymer powders. According to Figure 7, a decrease in bulk density occurred after a mixing time of 4 h, which is outside the standard deviation of the reference material. Therefore, a shorter mixing time is preferred. The limitation of the mixing time has been confirmed by various studies [43,45–47,49], which all consider a mixing time of a few minutes up to 1 h to be suitable. In order to achieve a sufficiently long mixing time without influencing the powder characteristics at the same time, a mixing time of 1 h is preferred. Although the mixing intensity has no measurable influence on the characteristics of the powder at a mixing time of 1 h, a minimum mixing intensity of 15 rpm is preferred in order to achieve the gentlest mixing of polymer powders. The limitation of the mixing intensity is also consistent with various studies [43,47,48]. Regarding a comparable resulting mixing energy, other combinations of mixing duration and mixing intensity can also be evaluated as suitable, as long as the mixing duration of 1 h is not exceeded.

## 4. Conclusions and Outlook

In order to compensate the influence on material characteristics and component properties due to ageing effects, powder already being used in the process is refreshed by adding new powder [4,11,24,51,52]. Basically, the fraction-based mixing of a defined ratio of new to recycled powder mentioned in Gibson et al. [2] must therefore be preceded by the selection of suitable mixing parameters. The aim of the work was to investigate the influence of the mixing parameters on the powder characteristics and to identify parameters that are gentle on the mixed material. The focus of the investigation was on the particle shape and PSD as well as on the bulk and tap density. The key conclusions are summarized as follows:

- A tumbling mixer for gentle mixing of a selected polyamide 12 sintering material was identified;
- The sphericity and aspect ratio increased with rising mixing energy by up to 1%. The mixing intensity had the stronger influence on the form factors than the mixing duration. Low mixing energies did not lead to any measurable change in the form factors;
- The particle size increased with rising mixing energy due to the formation of agglomerates, while the fine particle fraction decreased. In particular, mixing durations of 48 h and upwards resulted in an increased particle size of up to 4%. Low mixing durations did not measurably influence the particle size;
- The powder density decreased primarily with increasing mixing time. Here, the bulk density was more strongly influenced than the tap density. Starting from a mixing duration of 4 h and a mixing intensity of 44 rpm, there was a change in the powder

density that lies outside the standard deviation of the reference material. For mixing durations of more than 48 h, the mixing intensity also had an influence. The powder density was influenced by growing particle agglomerates and deformations;

- A maximum mixing time of 1 h and a maximum mixing intensity of 15 rpm are considered to be suitable for the mixing of polyamide 12 sintering material. The mixing parameters caused a decrease of the bulk and tap density of maximum 1.5% and an increase of the particle size characteristics of maximum 2%. The form factors were influenced by less than 1%;
- The mixing time of 1 h and the mixing intensity of 15 rpm ensured that the powders were mixed homogeneously and gently.

However, even if the investigations carried out ensure that the powder fractions are mixed in a way that is gentle on the mixed material, this work creates opportunities for further investigations. In order to validate the result and confirm the increase of the form factors, further investigations with higher mixing energies have to be carried out. In addition to the analysis of bulk density and tap density, further investigation methods for the analysis of the powder flow could also be considered. Various possibilities for determining the powder flow were mentioned in Schulze [14]. Although an influence trend of the mixing parameters can be recognized for almost all investigated powder properties, the change of the properties at low mixing energies is predominantly within the standard deviation. Future studies with more extensive sample size could manifest the validity of the results. Furthermore, it is necessary to investigate the influence of the mixing process on the expression and degradation of stabilizers and additives in the powder [11] as well as on the triboelectric properties of the powder [71,72]. It is also required to investigate the influence of the identified mixing parameters, which are gentle on the mixed material, on the powder and component properties during the cyclic reuse of the powder in the SLS process. As a result, further conclusions can be drawn about the degree of homogeneity of the powder mixture and the preservation of the mixed material during cyclic, fraction-based mixing.

**Author Contributions:** T.E.: Conceptualization, methodology, validation, formal analysis, investigation, project administration, resources, data curation, writing—original draft preparation, writing—review and editing, visualization; H.R.: Methodology, formal analysis, investigation; F.v.L.: Conceptualization, project administration, resources, supervision, validation, writing—review and editing. All authors have read and agreed to the published version of the manuscript.

**Funding:** This research received no external funding.

**Institutional Review Board Statement:** Not applicable.

**Informed Consent Statement:** Not applicable.

**Data Availability Statement:** Not applicable.

**Conflicts of Interest:** The authors declare no conflict of interest. The results, opinions and conclusions expressed in this publication are not necessarily those of Volkswagen Aktiengesellschaft.

## References

1. Seppala, J.E.; Kotula, A.P.; Snyder, C.R. *Polymer-Based Additive Manufacturing: Recent Developments*; American Chemical Society: Washington, DC, USA, 2019; ISBN 9780841234260.
2. Gibson, I.; Rosen, D.; Stucker, B. *Additive Manufacturing Technologies: 3D Printing, Rapid Prototyping and Direct Digital Manufacturing*, 2nd ed.; Springer: Berlin/Heidelberg, Germany, 2015; ISBN 978-1-4939-2112-6.
3. Celik, E. *Additive Manufacturing*; De Gruyter: Berlin, Germany, 2020; ISBN 9781501518782.
4. Choren, J.; Gervasi, V.; Herman, T.; Kamara, S.; Mitchell, J. SLS powder life study. In Proceedings of the 2001 Solid Freeform Fabrication Symposium, Austin, TX, USA, 6–8 August 2001; pp. 39–45.
5. Dahlmann, R.; Haberstroh, E.; Menges, G. *Menges Werkstoffkunde Kunststoffe, Vollständig Neu Bearbeitete Auflage*, 7th ed.; Hanser: Munich, Germany, 2022; ISBN 978-3-446-45801-7.
6. *DIN 50035:2012-09*; Begriffe auf dem Gebiet der Alterung von Materialien—Polymere Werkstoffe. Beuth Verlag GmbH: Berlin, Germany, 2012.
7. Dotchev, K.; Yusoff, W. Recycling of polyamide 12 based powders in the laser sintering process. *Rapid Prototyp. J.* **2009**, *15*, 192–203. [CrossRef]

8. Drummer, D.; Harder, R.G.; Witt, G.; Wegner, A.; Wudy, K.; Drexler, M. Long-term Properties of Laser Sintered Parts of Polyamide 12—Influence of Storage Time and Temperature on the Aging Behavior. *Int. J. Recent Contrib. Eng. Sci. IT* **2015**, *3*, 20. [CrossRef]
9. Kuehnlein, F.; Drummer, D.; Rietzel, D.; Seefried, A. Degradation behavior and material properties of PA 12 plastic powders processed by powder based additive manufacturing technologies. In *Annals of DAAAM for 2010 & Proceedings of the 21st International DAAAM Symposium*; DAAAM International Vienna: Vienna, Austria, 2010; Volume 21, pp. 1–2.
10. Huber, W. *Industrie 4.0 Kompakt—Wie Technologien unsere Wirtschaft und unsere Unternehmen Verändern: Transformation und Veränderung des Gesamten Unternehmens*; Springer: Berlin/Heidelberg, Germany, 2018; ISBN 978-3-658-20798-4.
11. Schmid, M. *Selektives Lasersintern (SLS) mit Kunststoffen: Technologie, Prozesse und Werkstoffe*; Hanser: München, Germany, 2015; ISBN 978-3-446-44562-8.
12. Schmid, M.; Amado, A.; Wegener, K. Polymer powders for selective laser sintering (SLS). In Proceedings of the PPS-30: The 30th International Conference of the Polymer Processing Society—Conference Papers, Cleveland, OH, USA, 6–12 June 2014; AIP Publishing LLC: Melville, NY, USA, 2015; p. 160009.
13. Schmid, M.; Wegener, K. Additive Manufacturing: Polymers Applicable for Laser Sintering (LS). *Procedia Eng.* **2016**, *149*, 457–464. [CrossRef]
14. Schulze, D. *Pulver und Schüttgüter*; Springer: Berlin/Heidelberg, Germany, 2019; ISBN 978-3-662-58775-1.
15. Schatt, W.; Kieback, B.; Wieters, K.-P. (Eds.) *Pulvermetallurgie: Technologien und Werkstoffe, Bearbeitete und Erweiterte Auflage*, 2nd ed.; Springer: Berlin/Heidelberg, Germany, 2007; ISBN 978-3-540-23652-8.
16. Masuda, H.; Higashitani, K.; Yoshida, H. *Powder Technology: Fundamentals of Particles, Powder Beds, and Particle*; CRC Press: Boca Raton, FL, USA, 2019; ISBN 9780367389802.
17. Mys, N.; Verberckmoes, A.; Cardon, L. Expanding the material palette for Selective Laser Sintering: Two production techniques for spherical powders. In *PMI 2018: 8th Bi-Annual International Conference on Polymers and Moulds Innovations*; Pontes, A., Ed.; Institute of Polymers and Composites, University of Minho: Guimaraes, Portugal, 2018; p. 7. ISBN 9789892088099.
18. Hirschberg, C.; Sun, C.C.; Risbo, J.; Rantanen, J. Effects of Water on Powder Flowability of Diverse Powders Assessed by Complimentary Techniques. *J. Pharm. Sci.* **2019**, *108*, 2613–2620. [CrossRef] [PubMed]
19. Faqih, A.M.N.; Mehrotra, A.; Hammond, S.V.; Muzzio, F.J. Effect of moisture and magnesium stearate concentration on flow properties of cohesive granular materials. *Int. J. Pharm.* **2007**, *336*, 338–345. [CrossRef] [PubMed]
20. *VDI 3405-Blatt 1: Additive Fertigungsverfahren-Rapid Manufacturing-Laser-Sintern von Kunststoffbauteilen-Güteüberwachung*; Beuth Verlag GmbH: Berlin, Germany, 2012.
21. Heugel, M.; Shellabear, M.; Pawliczek, S.; Maier, H. Method and System for Recycling Remaining Powder of an Equipment for Generatively Manufacturing Three-Dimensional Objects. U.S. Patent Application No.12/657,426, 5 August 2010.
22. Breuninger, J.; Becker, R.; Wolf, A.; Rommel, S.; Verl, A. *Generative Fertigung mit Kunststoffen: Konzeption und Konstruktion für Selektives Lasersintern*; Springer: Berlin/Heidelberg, Germany, 2013; ISBN 978-3-642-24324-0.
23. Gebhardt, A. *Additive Fertigungsverfahren: Additive Manufacturing und 3D-Drucken für Prototyping-Tooling-Produktion, neu Bearbeitete und Erweiterte Auflage*, 5th ed.; Hanser: München, Germany, 2016; ISBN 978-3-446-44401-0.
24. Josupeit, S.; Lohn, J.; Hermann, E.; Gessler, M.; Tenbrink, S.; Schmid, H.-J. Material Properties of Laser Sintered Polyamide 12 as Function of Build Cycles Using Low Refresh Rates. In Proceedings of the 26th Annual International Solid Freeform Fabrication Symposium, Austin, TX, USA, 10–12 August 2015; pp. 540–549.
25. Wegner, A.; Mielicki, C.; Grimm, T.; Gronhoff, B.; Witt, G.; Wortberg, J. Determination of Robust Material Qualities and Processing Conditions for Laser Sintering of Polyamide 12. *Polym. Eng. Sci.* **2014**, *54*, 1540–1554. [CrossRef]
26. Wegner, A.; Witt, G. Betrachtung zur Pulvernutzungsdauer beim Laser-Sintern und Einfluss der Prozessführung auf die Entstehung von Ausschussbauteilen. In *RTejournal-Forum für Rapid Technologie*; Aachen University of Applied Sciences: Aachen, Germany, 2012.
27. Pham, D.; Dotchev, K.; Yusoff, W. Deterioration of polyamide powder properties in the laser sintering process. *Proc. Inst. Mech. Eng. Part C J. Mech. Eng. Sci.* **2008**, *222*, 2163–2176. [CrossRef]
28. Rüsenberg, S.; Weiffen, R.; Knoop, F.C.; Schmid, H.-J.; de Gessler, M.; Pfisterer, H. Controlling the Quality of Laser Sintered Parts Along the Process Chain. In Proceedings of the 2012 23rd International Solid Freeform Fabrication Symposium (SFF 2012), Austin, TX, USA, 6–8 August 2012; pp. 1024–1044.
29. Kühnlein, F.; Drummer, D.; Wudy, K.; Drexler, M. Alterungsmechanismen der Kunststoffpulvern bei der Verarbeitung und deren Einfluss auf prozessrelevante Materialeigenschaften. *Ind. Des Sonderforschungsbereichs* **2012**, *814*, 49–66.
30. Drummer, D.; Kühnlein, F.; Rietzel, D.; Hülder, G. Untersuchung der Materialalterung bei pulverbasierten Schichtbauverfahren. In *RTejournal-Forum für Rapid Technologie*; Aachen University of Applied Sciences: Aachen, Germany, 2010.
31. Gornet, T. Materials and process control for rapid manufacture. In *Rapid Manufacturing: An Industrial Revolution for the Digital Age*; John Wiley & Sons: Chichester, UK, 2006; pp. 125–146.
32. Gornet, T.J.; Davis, K.R.; Starr, T.L.; Mulloy, K.M. Characterization of Selective Laser Sintering™ Materials to Determine Process Stability. In Proceedings of the 2002 International Solid Freeform Fabrication Symposium, Austin, TX, USA, 5–7 August 2002; pp. 546–553.
33. Drummer, D.; Wudy, K.; Drexler, M. Influence of energy input on degradation behavior of plastic components manufactured by selective laser melting. *Phys. Procedia* **2014**, *56*, 176–183. [CrossRef]

34. Pham, D.; Dotchev, K.; Yusoff, W. Improvement of part surface finishing in laser sintering by experimental design optimisation (DOE). In Proceedings of the Third Virtual International Conference on Innovative Production Machines and Systems (IPROMS 2007), 2–13 July 2007.
35. Bauman, I.; Ćurić, D.; Boban, M. Mixing of solids in different mixing devices. *Sadhana* **2008**, *33*, 721–731. [CrossRef]
36. Mwania, F.M.; Maringa, M.; van der Walt, K. Mixing and Reuse of Polymer Laser Sintering Powders to Ensure Homogeneity—A Review. *Int. J. Eng. Res. Technol.* **2020**, *13*, 3335. [CrossRef]
37. Deveswaran, R.; Bharath, S.; Basavaraj, B.V.; Abraham, S.; Furtado, S.; Madhavan, V. Concepts and techniques of pharmaceutical powder mixing process: A current update. *Res. J. Pharm. Technol.* **2009**, *2*, 245–249.
38. Stieß, M. *Mechanische Verfahrenstechnik-Partikeltechnologie 1*; Springer: Berlin/Heidelberg, Germany, 2009; ISBN 978-3-540-32551-2.
39. Sommer, K. Mechanismen des Pulvermischens. *Chem. Ing. Tech.* **1977**, *49*, 305–311. [CrossRef]
40. Weinekötter, R.; Gericke, H. *Mischen von Feststoffen: Prinzipien, Verfahren, Mischer*; Springer: Berlin/Heidelberg, Germany, 1995; ISBN 978-3-540-58567-1.
41. Bhoite, K.; Kakandikar, G.M.; Nandedkar, V.M. Schatz Mechanism with 3D-Motion Mixer—A Review. *Mater. Today Proc.* **2015**, *2*, 1700–1706. [CrossRef]
42. Weber, S. Untersuchungen zum Einfluss der Mischintensität auf die Potenz nanostrukturierter Fließregulierungsmittel. Ph.D. Thesis, Julius-Maximilians-Universität Würzburg, Würzburg, Germany, 2009.
43. Blümel, C. *Charakterisierung der Trockenen Beschichtung zur Herstellung von maßgeschneiderten Kompositpartikeln*; Universität Erlangen-Nürnberg: Erlangen, Germany, 2015; ISBN 978-3-8439-2120-6.
44. Fahr, A.; Voigt, R. *Voigt Pharmazeutische Technologie: Für Studium und Beruf*, 12th ed.; Deutscher Apotheker-Verlag: Stuttgart, Germany, 2015; ISBN 978-3-7692-6194-3.
45. Hogg, R. Mixing and Segregation in Powders: Evaluation, Mechanisms and Processes. *KONA* **2009**, *27*, 3–17. [CrossRef]
46. Poux, M.; Fayolle, P.; Bertrand, J.; Bridoux, D.; Bousquet, J. Powder mixing: Some practical rules applied to agitated systems. *Powder Technol.* **1991**, *68*, 213–234. [CrossRef]
47. Mayer-Laigle, C.; Gatumel, C.; Berthiaux, H. Mixing dynamics for easy flowing powders in a lab scale Turbula ®mixer. *Chem. Eng. Res. Des.* **2015**, *95*, 248–261. [CrossRef]
48. Ferraris, C.F. Concrete Mixing Methods and Concrete Mixers: State of the Art. *J. Res. Natl. Inst. Stand. Technol.* **2001**, *106*, 391–399. [CrossRef]
49. Shad, A.; Stache, R.; Rütjes, A. Effects of fumed silica flow aids on flowability and packing of metal powders used in Binder-Jetting additive manufacturing process. *Mater. Des.* **2021**, *212*, 110253. [CrossRef]
50. Musha, H.; Chandratilleke, G.R.; Chan, S.L.I.; Bridgwater, J.; Yu, A.B. Effects of size and density differences on mixing of binary mixtures of particles. In *Powders and Grains 2013, Proceedings of the 7th International Conference on Micromechanics of Granular Media, Sydney, Australia, 8–12 July 2013*; American Institute of Physics: College Park, MD, USA; pp. 739–742.
51. Fiedler, L.; Androsch, R.; Mileva, D.; Radusch, H.J.; Wutzler, A.; Gerken, J. Experimentelle Simulation der physikalischen Alterung von Lasersinterpulvern. *Z. Kunstst.* **2010**, *6*, 19–32.
52. Wudy, K.; Drummer, D.; Kühnlein, F.; Drexler, M. Influence of degradation behavior of polyamide 12 powders in laser sintering process on produced parts. In *PPS-29, Proceedings of the The 29th International Conference of the Polymer Processing Society-Conference Papers, Nuremberg, Germany, 15–19 July 2013*; American Institute of Physics: College Park, MD, USA, 2014; pp. 691–695.
53. Dadbakhsh, S.; Verbelen, L.; Verkinderen, O.; Strobbe, D.; van Puyvelde, P.; Kruth, J.-P. Effect of PA12 powder reuse on coalescence behaviour and microstructure of SLS parts. *Eur. Polym. J.* **2017**, *92*, 250–262. [CrossRef]
54. Amado, A.; Schmid, M.; Levy, G.; Wegener, K. Advances in SLS powder characterization. In Proceedings of the 22nd Annual International Solid Freeform Fabrication Symposium-An Additive Manufacturing Conference, SFF 2011, Austin, TX, USA, 8–10 August 2011.
55. Goodridge, R.D.; Tuck, C.J.; Hague, R. Laser sintering of polyamides and other polymers. *Prog. Mater. Sci.* **2012**, *57*, 229–267. [CrossRef]
56. Jonat, S.; Hasenzahl, S.; Drechsler, M.; Albers, P.; Wagner, K.; Schmidt, P. Investigation of compacted hydrophilic and hydrophobic colloidal silicon dioxides as glidants for pharmaceutical excipients. *Powder Technol.* **2004**, *141*, 31–43. [CrossRef]
57. Carr, J.F.; Walker, D.M. An annular shear cell for granular materials. *Powder Technol.* **1968**, *1*, 369–373. [CrossRef]
58. Carr, R.L., Jr. Evaluating flow properties of solids. *Chem. Eng.* **1965**, *18*, 163–168.
59. Spierings, A.B.; Voegtlin, M.; Bauer, T.; Wegener, K. Powder flowability characterisation methodology for powder-bed-based metal additive manufacturing. *Prog. Addit. Manuf.* **2016**, *1*, 9–20. [CrossRef]
60. Mullarney, M.P.; Beach, L.E.; Davé, R.N.; Langdon, B.A.; Polizzi, M.; Blackwood, D.O. Applying dry powder coatings to pharmaceutical powders using a comil for improving powder flow and bulk density. *Powder Technol.* **2011**, *212*, 397–402. [CrossRef]
61. Abdullah, E.C.; Geldart, D. The use of bulk density measurements as flowability indicators. *Powder Technol.* **1999**, *102*, 151–165. [CrossRef]
62. Zhou, Q.; Qu, L.; Larson, I.; Stewart, P.J.; Morton, D.A. Effect of mechanical dry particle coating on the improvement of powder flowability for lactose monohydrate: A model cohesive pharmaceutical powder. *Powder Technol.* **2011**, *207*, 414–421. [CrossRef]
63. *DIN EN ISO 60:2000-01*; Kunststoffe_-Bestimmung der scheinbaren Dichte von Formmassen, die durch einen genormten Trichter abfließen können (Schüttdichte) (ISO_60:1977). Deutsche Fassung EN_ISO_60:1999; Beuth Verlag GmbH: Berlin, Germany, 2000.

64. *DIN EN ISO 787-11:1995-10*; Allgemeine Prüfverfahren für Pigmente und Füllstoffe_- Teil_11: Bestimmung des Stampfvolumens und der Stampfdichte (ISO_787-11:1981). Deutsche Fassung EN_ISO_787-11:1995; Beuth Verlag GmbH: Berlin, Germany, 1995.
65. *ISO 13322-2:2021-12*; Particle Size Analysis-Image Analysis Methods-Part 2: Dynamic Image Analysis Methods. International Organization of Standardization: Vernier, Geneva, Switzerland, 2021.
66. Wadell, H. Volume, Shape, and Roundness of Quartz Particles. *J. Geol.* **1935**, *43*, 250–280. [CrossRef]
67. Frick, A.; Stern, C. *Einführung in die Kunststoffprüfung: Prüfmethoden und Anwendungen*; Hanser: München, Germany, 2017; ISBN 978-3-446-44351-8.
68. Seul, T. Ansätze zur Werkstoffoptimierung beim Laserintern durch Charakterisierung und Modifizierung grenzflächenenergetischer Phänomene: Approach for optimizing material for lasersintering by means of characterisation and modification interfacial-energy-phenomenon. Ph.D. Thesis, RWTH Aachen, Aachen, Germany, 2004.
69. Rietzel, D. Werkstoffverhalten und Prozessanalyse beim Laser-Sintern von Thermoplasten. Ph.D. Thesis, Friedrich-Alexander-Universität Erlangen-Nürnberg, Erlangen-Nürnberg, Germany, 2011.
70. Forsyth, A.; Hutton, S.; Rhodes, M. Effect of cohesive interparticle force on the flow characteristics of granular material. *Powder Technol.* **2002**, *126*, 150–154. [CrossRef]
71. Hesse, N.; Dechet, M.A.; Bonilla, J.S.G.; Lübbert, C.; Roth, S.; Bück, A.; Schmidt, J.; Peukert, W. Analysis of tribo-charging during powder spreading in Selective Laser Sintering: Assessment of polyamide 12 powder ageing effects on charging behavior. *Polymers* **2019**, *11*, 609. [CrossRef] [PubMed]
72. Schmidt, J.; Dechet, M.A.; Gómez Bonilla, J.S.; Hesse, N.; Bück, A.; Peukert, W. Characterization of polymer powders for selective laser sintering. In Proceedings of the 2019 International Solid Freeform Fabrication Symposium, Austin, TX, USA, 12–14 August 2019; pp. 779–789.